



Equilibrium shoreline response: Observations and modeling

M. L. Yates,¹ R. T. Guza,¹ and W. C. O'Reilly¹

Received 5 March 2009; revised 23 June 2009; accepted 6 July 2009; published 18 September 2009.

[1] Shoreline location and incident wave energy, observed for almost 5 years at Torrey Pines beach, show seasonal fluctuations characteristic of southern California beaches. The shoreline location, defined as the cross-shore position of the mean sea level contour, retreats by almost 40 m in response to energetic winter waves and gradually recovers during low-energy summer waves. Hourly estimates of incident wave energy and weekly to monthly surveys of the shoreline location are used to develop and calibrate an equilibrium-type shoreline change model. By hypothesis, the shoreline change rate depends on both the wave energy and the wave energy disequilibrium with the shoreline location. Using calibrated values of four model free parameters, observed and modeled shoreline location are well correlated at Torrey Pines and two additional survey sites. Model free parameters can be estimated with as little as 2 years of monthly observations or with about 5 years of ideally timed, biannual observations. Wave energy time series used to calibrate and test the model must resolve individual storms, and model performance is substantially degraded by using weekly to monthly averaged wave energy. Variations of free parameter values between sites may be associated with variations in sand grain size, sediment availability, and other factors. The model successfully reproduces shoreline location for time periods not used in tuning and can be used to predict beach response to past or hypothetical future wave climates. However, the model will fail when neglected geologic factors are important (e.g., underlying bedrock limits erosion or sand availability limits accretion).

Citation: Yates, M. L., R. T. Guza, and W. C. O'Reilly (2009), Equilibrium shoreline response: Observations and modeling, *J. Geophys. Res.*, 114, C09014, doi:10.1029/2009JC005359.

1. Introduction

[2] Sandy beaches erode and accrete in response to changing wave conditions. Models for wave-driven change in beach sand levels span a wide range from complex flux gradient models to simple bulk response models. Flux gradient models estimate changes in sand level using conservation of mass, with spatial gradients in time-averaged sediment flux balanced by erosion or accretion. At the detailed end of the flux-gradient-model spectrum are wave phase resolving, two-phase flow models that include both intergranular interactions and turbulent suspension in flux estimates [e.g., Dong and Zhang, 2002; Hsu et al., 2004]. These computationally intensive models predict time-dependent fluid velocities and sediment fluxes in the wave boundary layer and require input time series of velocity (including wave orbital velocity) above the wave boundary layer at many grid points. Values of several model coefficients are often unknown because many of the small-scale processes included are not well understood. Other flux gradient models empirically relate wave-averaged low-order moments (e.g., variance and skewness) of velocity and

acceleration to wave-induced seabed stresses and sediment transport. For example, skewness (or the third moment) of cross-shore velocity [Bailard, 1981] and cross-shore acceleration [Drake and Calantoni, 2001] time series have been used in morphologic change models (Roelvink and Stive [1989], Gallagher et al. [1998], Hoefel and Elgar [2003], and others). Similar to the more complex two-phase models, spatial gradients in the estimated sediment flux are balanced by erosion or accretion.

[3] Bulk response models are essentially phenomenological; observations of waves and beach change are used to validate and calibrate simple heuristic rules for beach change. Equilibrium profile models, one subset of bulk response models, suggest that a beach exposed to steady wave conditions will evolve toward a unique equilibrium beach profile. When this shape is reached, no further change occurs. Equilibrium shapes have been suggested, for example $h(x) = Ax^{2/3}$, where h is the water depth, x is the distance offshore, and A depends on sediment grain size (Bruun [1954], Dean [1977], and others). Alternative shapes for the equilibrium beach profile, with finite shoreline slope or the inclusion of offshore sandbars, have been proposed [e.g., Larson and Kraus, 1989; Inman et al., 1993; Özkan Haller and Brundidge, 2007]. Equilibrium beach response concepts have been used to model the evolution of beach profiles [Larson and Kraus, 1989] and nourishment projects [Dean, 1991], interannual variations in the cross-shore location of the sandbar crest [Plant et al., 1999], and

¹Scripps Institution of Oceanography, University of California, San Diego, La Jolla, California, USA.

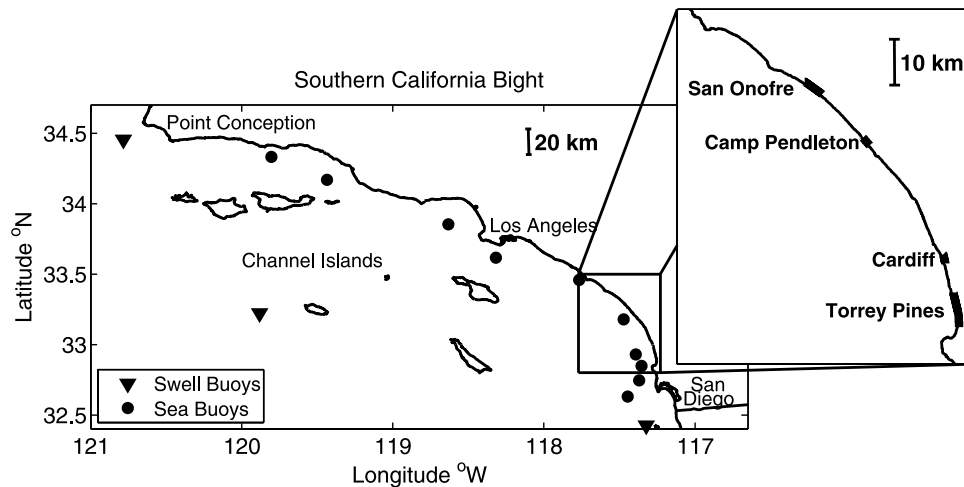


Figure 1. Map of Southern California Bight with wave buoy (see legend) and in situ survey (see inset) locations.

shoreline response to sea level rise [Dubois, 1990], storm surges [Kriebel and Dean, 1993], and storms [Miller and Dean, 2004].

[4] Wright and Short [1984] developed a conceptual set of equilibrium beach states, including straight and along-shore variable sandbars, which depend on the value of the Dean parameter, $\Omega = H_b/w_s T$ [Gourlay, 1968; Dean, 1973], where H_b is the breaking wave height, w_s is the grain-size-dependent sediment fall velocity, and T is the wave period. However, beach morphologies do not respond instantaneously to the changing wave field, and correlations between observed beach state and instantaneous Ω were weak. Morton et al. [1995], Lee et al. [1998], Anthony [1998], and Jiménez et al. [2008] further emphasize the observed low correlation between instantaneous wave conditions and beach state, on beaches dominated by storms with intermittent and seasonal recovery periods. For example, in a few hours during storm spin-up and spin-down, the wave field can vary far more rapidly than the morphology evolves.

[5] Wright et al. [1985] suggested that the present beach state is determined by the recent history of both the wave field and the beach morphology. Dalrymple [1992], Masselink and Short [1993], List and Farris [1999], Larson et al. [2000], Miller and Dean [2007], and Quartel et al. [2008], among others, used instantaneous or averaged wave properties to define transitions between beach states.

[6] Wright et al. [1985] further suggested that beaches progress toward an equilibrium state, which depends on the instantaneous disequilibrium of the wave field ($\Omega - \Omega_{eq}$) and the relative magnitude of the wave event (Ω or Ω^2), but they lacked sufficient observations to confirm this hypothesis. More recently, Miller and Dean [2004] developed a simple model relating shoreline change to the disequilibrium of the shoreline position, which depends on the wave conditions, water level (including storm surge, wave setup, and tides), and berm height. They formulate shoreline change as

$$\frac{dy(t)}{dt} = k(y_{eq}(t) - y(t)), \quad (1)$$

where y is the shoreline position, y_{eq} the equilibrium shoreline position, and k the rate constant, which can have different values for erosion and accretion. We pursue the equilibrium concepts of Wright et al. [1985] and Miller and Dean [2004] using extensive observations of shoreline location and hourly estimates of the wave field, which resolve even short-lived storms.

[7] At Torrey Pines State Beach in southern California, the site of the present study, seasonal erosion and accretion patterns were quantified with empirical eigenfunctions of monthly cross-shore profiles [Winant et al., 1975; Aubrey, 1979]. Aubrey et al. [1980] made statistical predictions of weekly profile eigenfunctions using a combination of the weekly averaged wave energy and the previous profile eigenfunction values as predictors including the effects of the instantaneous forcing and the antecedent beach state. Their suggestion that a longer data set and shorter wave-averaging interval would decrease the forecast error is confirmed by our results.

[8] Here, multiyear observations of shoreline position and incident waves at Torrey Pines beach (described in section 2) are used to qualitatively illustrate equilibrium beach change concepts (section 3). A simple equilibrium shoreline model is developed (section 4), which reproduces well the observed shoreline movement at Torrey Pines and two nearby survey sites (section 5). The effects of survey sampling frequency and duration on model performance, the strong relationship between the displacement of shoreline and other depth contours, and the general model applicability are discussed (section 6).

2. Observations

[9] Sand levels and waves were monitored at four study sites within a 65-km alongshore reach in San Diego County, California (Figure 1).

2.1. Study Sites

[10] The general survey site characteristics (e.g., beach slope, sand grain size) are summarized in Table 1. Torrey Pines (8 km) is a wide, sandy beach backed by a revetment

Table 1. Beach Width, Beach Slope at Msl, and Median Sand Grain Diameter at Msl and at Approximately +1 to +2 m Elevation for Each Survey Site^a

Survey Site	Beach Width (m)	Beach Slope	Msl D50 (mm)	+1 to +2 m D50 (mm)
Torrey Pines	20–120	0.01–0.03	0.23	0.18
Cardiff	20–50	0.02–0.04	0.16	–
Camp Pendleton	50–130	0.02–0.04	0.20	0.23
San Onofre	20–70	0.03–0.05	0.26	0.35

^aBeach width is the distance between msl and the backbeach, and the median sand grain diameter is D50.

in the northern section and approximately 100 m high cliffs in the southern section. Patches (10’s of meters alongshore) of a single layer of cobbles may appear on the beach face during winter. Approximately 15 km to the north, Cardiff (2 km) is a narrow, sandy beach with regions (100’s of meters alongshore) of exposed bedrock on the beach face and in the surf zone. The northern end of the beach is backed by a revetment, and the southern end is backed by cliffs (about 20 m high). Thin cobble layers (100’s of meters alongshore) often cover portions of the exposed beach face during winter months. Farther to the north, Camp Pendleton (2.5 km) is a wide, sandy beach, similar to Torrey Pines.

The beach is backed by vegetated dunes and remains sandy throughout the year. The northernmost survey site, San Onofre (4 km), is a narrow and steep beach. The upper portion of the beach face is exposed to wave action at high tide and is mostly covered in thick cobble cusps throughout the year. Shoreward of the cusps, a flat, silty and sandy region extends landward to the base of 40-m high cliffs. Neap and Spring tidal ranges at all sites are approximately 1.0 and 2.5 m, respectively.

2.2. Sand Level Observations

[11] Weekly to monthly surveys above the low tide waterline, spanning the subaerial beach, were acquired with a GPS-equipped all terrain vehicle (ATV) driven on shore-parallel transects, separated by approximately 10 m in the cross-shore direction (Figure 2b). Two to four times yearly full bathymetry surveys spanned from the backbeach (e.g., cliffs, revetment) to approximately –9 m water depth along predefined cross-shore transects (Figure 2a). During low tide the ATV and a hand-pushed cart surveyed to wading depths, and during high tide a personal watercraft with a GPS antenna and depth sounder surveyed from –9 m depth to the breaker line. At each survey site, more than 75% of the mean sea level (msl) observations were estimated from

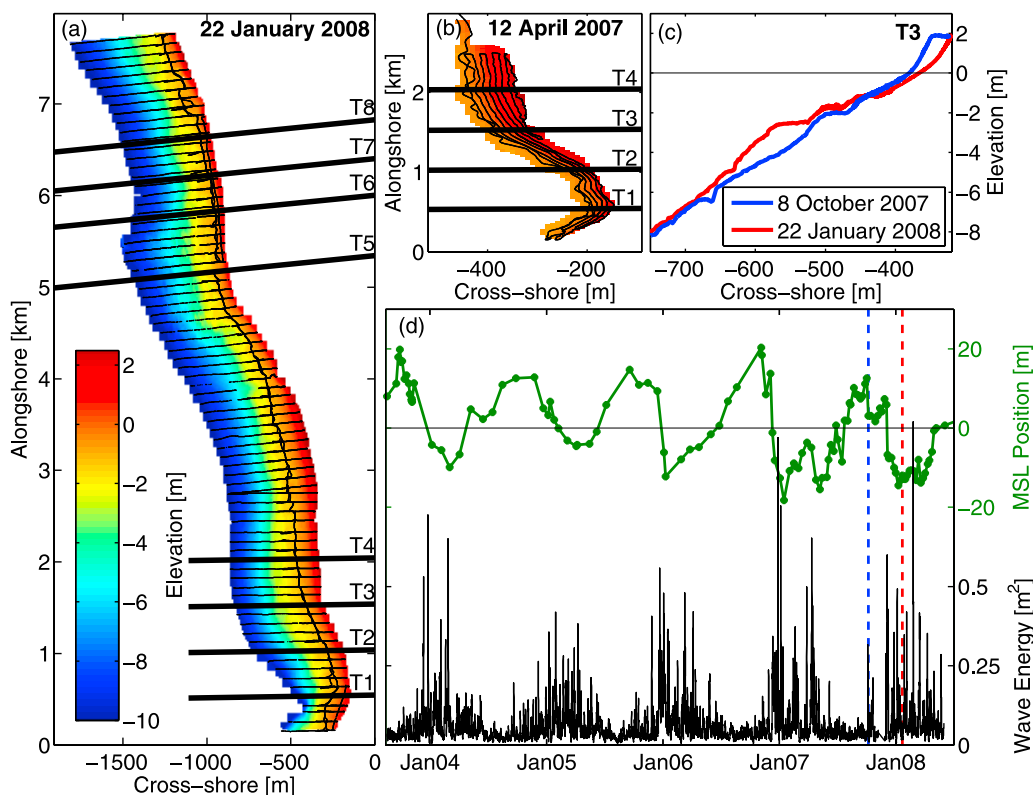


Figure 2. Torrey Pines bathymetry. (a) The 22 January 2008 full bathymetry survey, with thin black lines showing the survey tracks. Bold, black lines labeled T1–T8 (south to north) indicate the 500-m alongshore sections over which msl observations were averaged. (b) Southern 2-km reach of 12 April 2007 subaerial beach survey (approximately 0 to +2-m elevation), with thin black lines showing the survey tracks (depth color scale same as in Figure 2a). (c) Depth versus cross-shore location for a typical accreted and eroded beach (section T3), and (d) msl position with the temporal mean removed (green) and hourly wave energy (black) versus time. Dashed vertical lines indicate the survey dates of the cross-shore profiles shown in Figure 2c.

Table 2. Alongshore Survey Length, Survey Date Range, Number of Surveys, and Approximate Frequency of Surveys for Each Survey Site

Survey Site	Alongshore Length (km)	Date Range	Number of Surveys	Frequency of Alongshore Surveys
Torrey Pines	8	Dec 2002 to Jul 2008	134	weekly to monthly
Cardiff	2	May 2007 to Jul 2008	32	biweekly
Camp Pendleton	2.5	Dec 2006 to Jul 2008	26	monthly
San Onofre	4	May 2005 to Mar 2007	17	monthly ^a

^aSampled monthly until August 2006, with one additional survey in March 2007.

the frequent subaerial surveys (Figure 2b). Root-mean-square (RMS) vertical errors are estimated to be less than 15 cm. See Table 2 for survey details.

2.3. Wave Observations and Estimates

[12] In the Southern California Bight, the Channel Islands (Figure 1) shelter incoming wave energy creating wave shadows along the coastline [Pawka, 1983]. A spectral refraction wave model [O'Reilly and Guza, 1998], which resolves the island shadows and refraction over offshore bathymetry, is used to estimate the hourly directional wave properties every 100 m alongshore at the -10 m depth contour. Swell waves (0.04–0.1 Hz) are initialized with buoys (solid triangles, Figure 1) exposed to the open ocean, located seaward of the Channel Islands within a 400-km radius, and sea waves (0.08–0.5 Hz) are initialized with nearshore buoys (solid circles, Figure 1) located within a 75-km radius of the prediction location.

3. Equilibrium Change Observations

[13] Beach sand level changes and waves are first related qualitatively using the extensive multiyear observations at Torrey Pines beach. Monthly (or more frequent) subaerial surveys of two approximately 2-km reaches were separated into eight 500-m alongshore sections (T1–T8, south to north, Figure 2a). To facilitate integration with the full bathymetry surveys, msl position was determined along the predefined cross-shore transects spaced approximately every 100 m alongshore. Changes in msl location were calculated on each transect and then averaged within each 500-m alongshore section. The temporal mean msl position for each 500-m section (beach width range in Table 1) was removed, yielding time series of msl position fluctuations about the mean (Figure 2d, msl position). Mean hourly wave energy was obtained by averaging the incident spectral wave energy estimates (at the -10 m depth contour), spaced every 100 m alongshore, over each 500-m section (Figure 2d, wave energy).

[14] In all eight sections, msl position and wave energy show large seasonal cycles. The wave energy is typically low during summer, with episodic, high-energy winter storms. At all alongshore locations, the beach is most accreted (positive msl position) after continuous, low-energy summer waves, and the beach is most eroded (negative msl position) after episodic, high wave energy winter storms. Msl position and wave energy statistics vary relatively little in the alongshore between most 500-m sections. Section T3 is representative and is shown in Figures 2c, 2d, 4, 5, 8, 9, 11, 13, 14, and 15.

[15] Time series of instantaneous msl position S and average wave energy \bar{E} (where the overbar denotes the

average between successive surveys) are only weakly correlated ($R^2 < 0.14$ for all alongshore sections). However, consistent with equilibrium concepts, the msl change rate dS/dt does depend on \bar{E} for a given initial S (Figure 3). Eroding and accreting waves are separated by the equilibrium energy \bar{E}_{eq} (calculated using data averaged between successive surveys), which causes no msl change for a particular initial msl position (black line at blue-red boundary, Figure 3). The equilibrium energy depends on the initial msl position; therefore, the shoreline response will vary for two events with the same wave energy but different initial msl position. For example, a moderate wave energy of about 0.05 m^2 ($H_{sig} = 0.9 \text{ m}$), which erodes an accreted beach (positive msl, Figure 3) can accrete an eroded beach (negative msl, Figure 3). Larger wave energy events are required to continue eroding an already eroded beach. The msl change rate appears to increase when wave energy is farther from the equilibrium wave energy (e.g., as the disequilibrium $\bar{E} - \bar{E}_{eq}$, the deviation from the solid line, increases (see color scale in Figure 3)).

4. Model

[16] The beach response at Torrey Pines (Figure 3) suggests a simple equilibrium-type model. Following the concepts of Wright *et al.* [1985], the instantaneous msl change rate is assumed proportional to both the instantaneous energy E and the instantaneous energy disequilibrium ΔE for the current msl position

$$\frac{dS}{dt} = C^\pm E^{1/2} \Delta E, \quad (2)$$

where C^\pm are change rate coefficients for accretion (C^+ for $\Delta E < 0$) and erosion (C^- for $\Delta E > 0$), and the energy disequilibrium is

$$\Delta E(S) = E - E_{eq}(S). \quad (3)$$

[17] The equilibrium wave energy E_{eq} depends on the initial msl position S , and the sign of the msl change rate dS/dt is determined by the sign of the energy disequilibrium ΔE . The factor $E^{1/2}$ prevents nonphysical changes in msl position when E is small and will be discussed further in section 6.1. For simplicity, we define the equilibrium wave energy as a linear function of the msl position

$$E_{eq}(S) = aS + b, \quad (4)$$

where a and b are the slope and y intercept, respectively (similar to the solid line (\bar{E}_{eq}) in Figure 3). That is, for a given msl position S there is an equilibrium wave energy

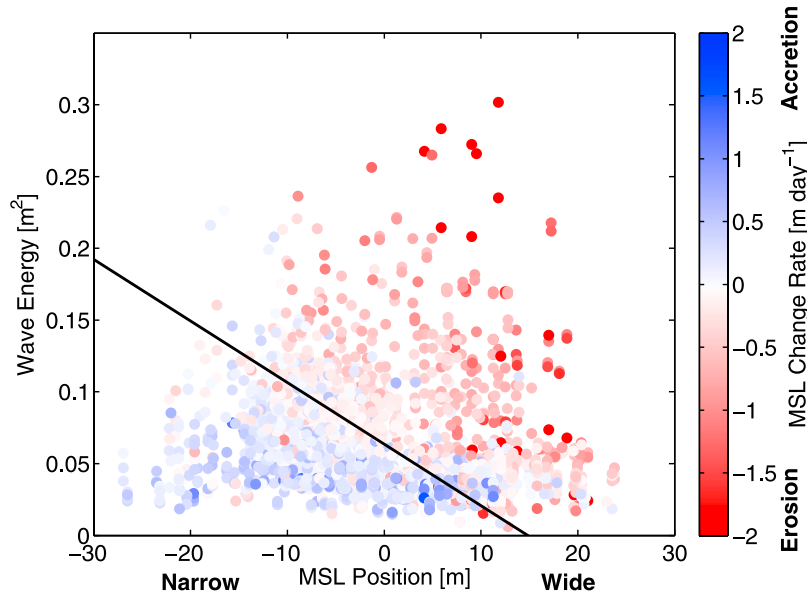


Figure 3. Msl change rate $\overline{dS/dT}$ between consecutive weekly and monthly surveys (shown in color) versus the initial msl position S and average energy between surveys \bar{E} , for all eight alongshore sections at Torrey Pines beach. The equilibrium wave energy \bar{E}_{eq} (solid line) is the best fit line (4) to the observed average wave energy causing no msl position change.

E_{eq} that causes no change. Rearranging (4) yields the equilibrium msl position for a given wave energy

$$S_{eq}(E) = \frac{E - b}{a}. \quad (5)$$

The equilibrium msl position would be obtained if the wave energy remained constant for an extended period of time, allowing the beach to equilibrate fully with the wave forcing.

[18] The model approaches equilibrium exponentially, as suggested by *Swart* [1974] and *Larson and Kraus* [1989] and similar to the equilibrium model of *Miller and Dean* [2004]. The model behavior is illustrated in the simple case when the time series of wave energy E is a step function, either increasing or decreasing to fixed level and remaining constant thereafter. In this case, the solution to (2)–(5) is

$$S(t) = (S_0 - S_{eq})e^{-aC^\pm E^{1/2}t} + S_{eq}, \quad (6)$$

where S_0 is the initial msl position, and for a fixed wave energy E , S_{eq} is the equilibrium msl position, which depends on a and b (5). With equal C^+ and C^- , the e-folding scale $[aC^\pm E^{1/2}]^{-1}$ shows faster adjustment to high-energy waves than to low-energy waves. Time scale estimates, based on the free parameters fit to the observations, are discussed below.

[19] The model has four free parameters: two coefficients [a and b , (4)] determining the equilibrium energy for an initial msl position, and the accretion and erosion rate coefficients [C^\pm , (2)]. Initially, a and b were determined from the observations using wave energy averaged over the period between successive surveys \bar{E} (solid line in Figure 3). The optimal C^\pm , yielding the minimum square

error between modeled and observed msl position, were then found explicitly by solving (2)–(4) using the observed initial S , and the averaged \bar{E} and $\overline{dS/dt}$ between surveys. However, weekly to monthly averaged wave energy \bar{E} unacceptably smoothed storm events and obscured the timing of storms within the averaging period (discussed further in section 6.6).

[20] Hourly wave energy estimates E resolve even rapidly varying wave conditions, and after the free parameters are determined, allow hourly updates of shoreline location (2). However, the many hour time steps (about 44,000 in 5 years) complicate the numerics of finding the best fit parameters in this nonlinear system. Two derivative-free techniques were used to solve for the four free parameters that minimize the root-mean-square error (RMSE) between the model and observations: simulated annealing [*Barth and Wunsch*, 1990] and surrogate management framework [*Booker et al.*, 1999; *Marsden et al.*, 2004]. Derivative-free methods are used because the present system has many local minima in the four-dimensional parameter space that can trap gradient methods. Simulated annealing and surrogate management framework (SMF) search the parameter space differently but yield similar results for test cases. SMF required significantly fewer cost function evaluations to minimize the RMSE, and SMF results are presented below.

5. Results

5.1. Torrey Pines

[21] The observed and modeled (using optimal model parameters) msl position both show strong seasonal variation, with slow accretion for long periods of low-energy waves, and faster erosion during episodic, high-energy wave events (e.g., Figure 4). Section T3 (Figure 4) is representative of all eight alongshore sections, which have RMSE ranging between 3.3 and 5.2 m.

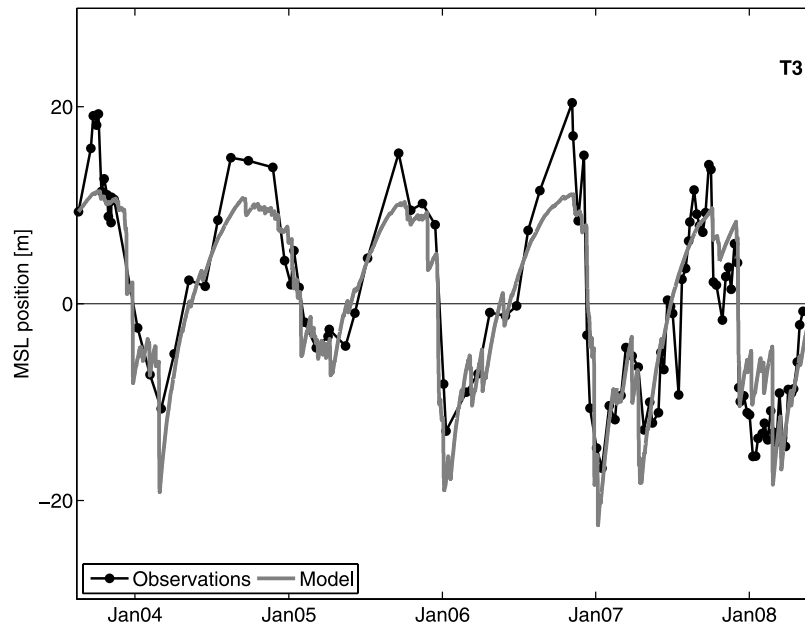


Figure 4. Weekly to monthly observations of msl position (with the temporal mean removed, black curve) and hourly model results (gray curve) versus time at Torrey Pines section T3 (RMSE = 4.0 m).

[22] The optimal erosion and accretion change rate coefficients C^{\pm} are of the same order of magnitude. The change potential $|E^{1/2}\Delta E|$, which is the product of the relative magnitude of the wave energy and the wave energy disequilibrium, accounts for much of the variability in the relative

size of erosion and accretion events (2) within each along-shore section. The change potential is consistently small for accretion, with larger, episodic spikes for erosion (Figure 5c). The modeled shoreline accretes between 60 and 90% of the year, depending on the year and alongshore location.

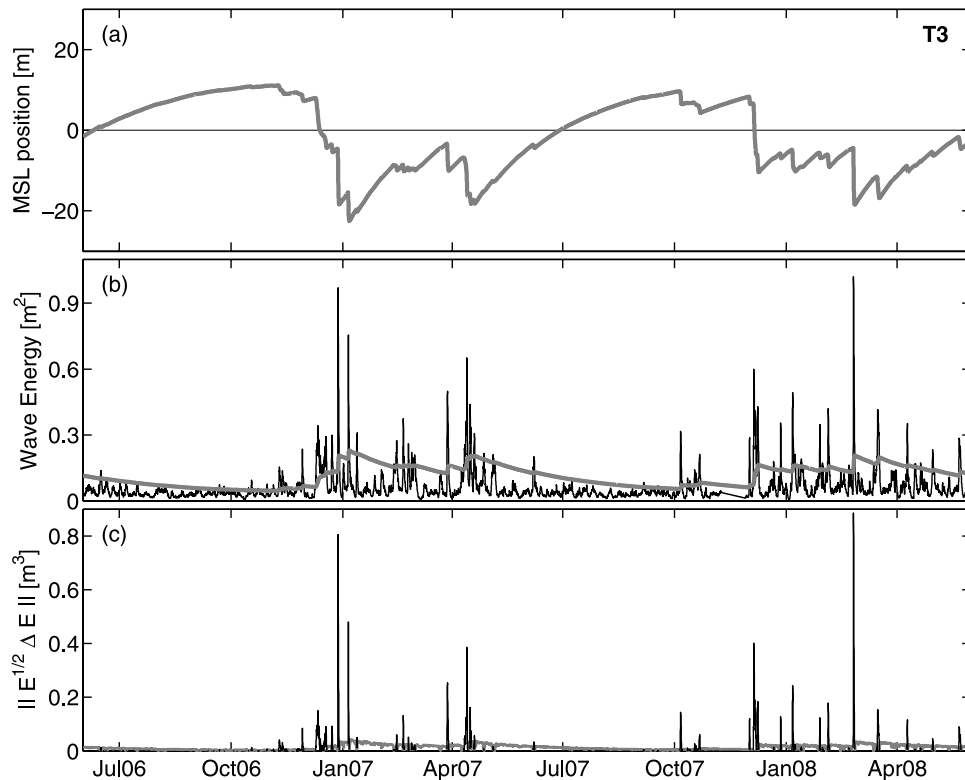


Figure 5. Two years at Torrey Pines section T3. (a) Modeled msl position, (b) observed wave energy E (black curve) and model equilibrium wave energy E_{eq} (gray curve), and (c) change potential $|E^{1/2}\Delta E|$, where $\Delta E = E - E_{eq}$, for accretion ($\Delta E < 0$, gray curve) and erosion ($\Delta E > 0$, black curve) events.

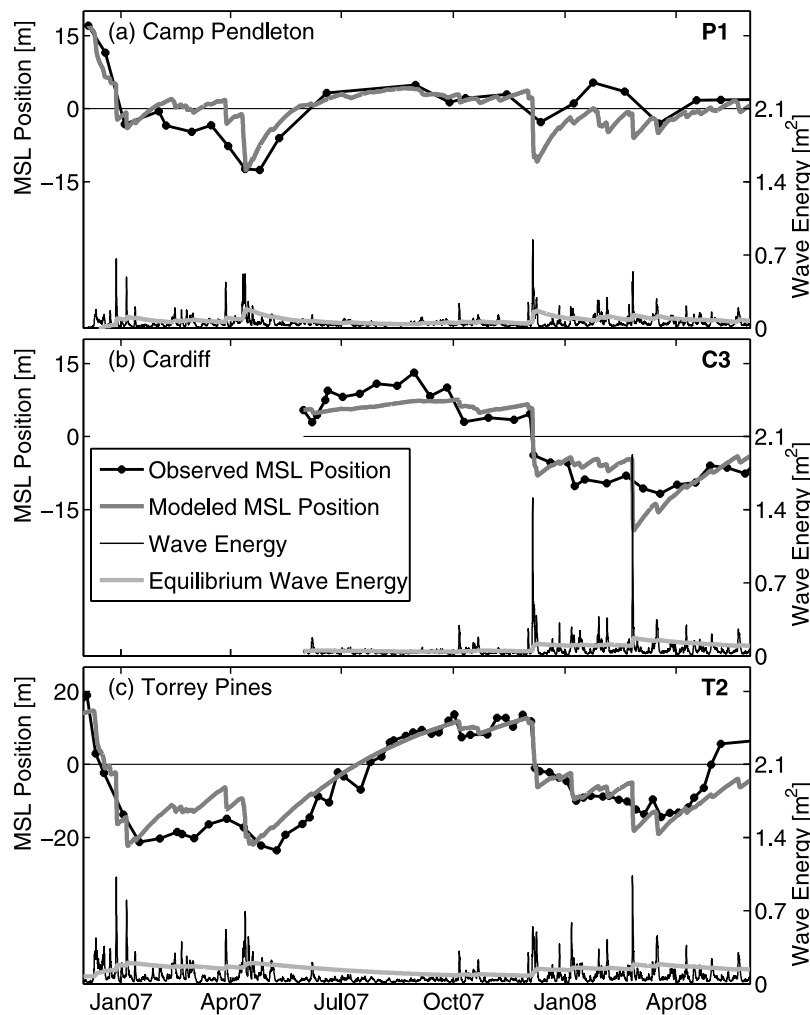


Figure 6. The top plot in each graph is the observed and modeled msl position (black and gray curves, respectively) and the bottom plot in each graph is the wave energy and equilibrium wave energy (black and gray curves, respectively) versus time at (a) Camp Pendleton section P1, (b) Cardiff section C3, and (c) Torrey Pines section T2. Model errors (RMSE) are 3.5, 2.9, and 4.0 m, respectively.

[23] The first winter storms cause the most pronounced erosion events because the wave energy disequilibrium and erosion change potential are large (Figure 5c). Although the wave energy E often may be elevated through the winter and early spring, accretion can occur (e.g., January–April 2007, Figure 5a) when moderate wave energy events E are smaller than the current equilibrium wave energy E_{eq} (gray line, Figure 5b).

[24] The e-folding scale $[aC^{\pm}E^{1/2}]^{-1}$ (6), calculated with the free parameters determined at Torrey Pines beach, ranges from approximately 1 to 3 weeks for strongly erosive events with high wave energy, to approximately 1–3 months for accretion events during lulls in wave energy, similar to estimates by *Miller and Dean* [2006]. Msl position time series are much smoother than the corresponding wave energy time series (Figure 5), consistent with equilibrium response times much longer than storm durations. In the summer months, the beach slowly approaches its maximum width $-b/a$ but does not equilibrate fully with the low-energy summer waves (E_{eq} , gray line, larger than E , black line,

Figure 5b) because the equilibration time scale is longer than the duration of low-energy waves.

5.2. Additional Sites

[25] The model was applied at three additional sites that were surveyed at least monthly for more than 1 year. Similar to Torrey Pines, the beaches were divided into 500-m alongshore sections, resulting in four sections at Cardiff, four sections at Camp Pendleton, and six sections at San Onofre (depending on the alongshore survey length).

[26] At Camp Pendleton and Cardiff, the model reproduces the observations with RMSE similar to Torrey Pines. With approximately 1.5 years of monthly beach surveys at Camp Pendleton, the RMSE ranges from 3.5 to 5.4 m for the four alongshore sections (section P1, Figure 6a). With slightly more than a year of biweekly observations at Cardiff, the RMSE ranges from 2.7 to 5.3 m for the four alongshore sections (section C3, Figure 6b). Monthly msl position observations at San Onofre (not shown) exhibit a weak, barely detectable seasonal cycle even though the

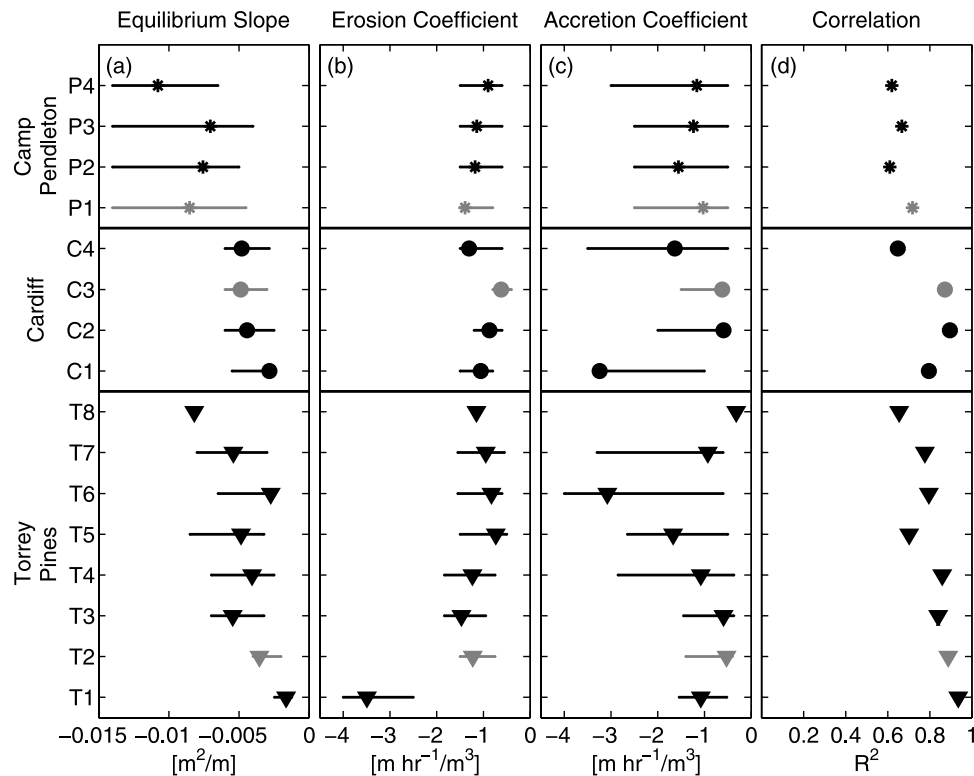


Figure 7. Optimal model free parameters at Torrey Pines, Cardiff, and Camp Pendleton for (a) equilibrium slope a (4), (b) erosion rate coefficient C^- , (c) accretion rate coefficient C^+ , and (d) squared correlation R^2 between modeled and observed msl position. Scatter bars indicate the range of free parameter values for which the RMSE increases by less than 10% from the minimum. Gray symbols indicate the alongshore sections shown in Figure 6.

seasonality of wave energy and the storm event magnitudes are similar to Camp Pendleton (20 km to the south). Coarse-grained sand on the beach face or limited sand availability in the nearshore zone are hypothesized to stabilize the shoreline at San Onofre. The small msl position changes (<5 m) were only slightly larger than the observation uncertainties, and the model performs poorly.

[27] At the three sites with significant seasonal msl change, the model performs well, and the correlation (R^2) between the observed and modeled msl position (using optimal parameter values for each section) is between 0.61 and 0.94 (Figure 7d). Average R^2 (over all 500-m alongshore sections) values are 0.81 (Torrey Pines), 0.65 (Camp Pendleton), and 0.80 (Cardiff). Thus, most of the variance in the observed msl time series can be explained by an equilibrium-type model driven with hourly waves resolving seasonal wave energy fluctuations including episodic storms.

[28] The range of free parameter values for which the RMSE between observed and modeled msl position increases less than 10% was estimated (Figure 7). The equilibrium y intercept b (not shown) depends on the temporal mean removed from the msl time series and is not comparable between different alongshore sections with variable temporal sampling. The values of the free parameters a and C^\pm are related and can have compensating effects that create broad RMSE minima in the free parameter space. For example, an increase in the magnitude of the equilibrium slope a (with b constant) increases the wave energy required to initiate erosion, thus causing fewer erosion events and correspond-

ingly more accretion. However, this change can be balanced by an increase in the erosion rate coefficient C^- (increasing the impact of the remaining erosion events) and a decrease in the accretion rate coefficient C^+ (decreasing the impact of the accretion events). Within each survey site, a single set of free parameters reproduces the observations at most alongshore locations with a less than $\sim 10\%$ increase in RMSE.

[29] The optimal free parameters vary between survey sites (Figure 7), but demonstrate similar equilibrium response (Figure 6). The equilibrium slope a (4) is consistently larger at Camp Pendleton than at Cardiff and most of Torrey Pines (Figure 7 and Table 3), indicating that the equilibrium msl position has a smaller range of values for the same range of wave conditions (5). The magnitude and range of the optimal erosion rate coefficient C^- shows relatively little variation between alongshore sections and survey sites (Table 3), with the exception of T1 (Figure 7b). The lowest wave energy and largest alongshore gradients in wave energy (not shown) are at T1, and alongshore transport divergence may be important.

[30] The accretion rate coefficients C^+ show larger variability and ranges of accepted values than the erosion rate coefficients C^- , both between and within sites (Figure 7c and Table 3). Accretion change potentials (gray curve, Figure 5c) are small and persistent, and a broad range of C^+ values have a similar impact on msl position change. If C^+ were increased (and all other free parameters remained the same), the msl position would more rapidly approach the equilibrium value during wave energy lulls, but the net amount of accretion would not increase significantly. In contrast, erosion events

Table 3. Mean and Standard Deviation of the Equilibrium Slope a , Erosion Rate Coefficient C^- , Accretion Rate Coefficient C^+ , and Products of aC^\pm for Each Survey Site

Survey Site	a ($\times 10^{-3}$ m ² /m)	C^- (m h ⁻¹ /m ³)	C^+ (m h ⁻¹ /m ³)	aC^- ($\times 10^{-3}$ m ⁻¹ h ⁻¹)	aC^+ ($\times 10^{-3}$ m ⁻¹ h ⁻¹)
Torrey Pines	-4.5 ± 2.0	-1.38 ± 0.88	-1.16 ± 0.88	5.4 ± 2.3	4.4 ± 2.6
Cardiff	-4.2 ± 1.0	-0.96 ± 0.29	-1.52 ± 1.25	4.0 ± 1.6	5.6 ± 3.3
Camp Pendleton	-8.5 ± 1.7	-1.15 ± 0.20	-1.24 ± 0.22	9.6 ± 1.6	10 ± 2.0

have much larger change potentials (black curve, Figure 5c) that persist only briefly but have a significant impact on msl position change, restricting the range of acceptable erosion rate coefficients C^- . Overall, the model is more sensitive to variations in C^- than C^+ .

[31] The e-folding scale from (6) shows that the rate of adjustment to equilibrium depends on aC^\pm [m⁻¹ h⁻¹] and the magnitude of the wave event. Camp Pendleton has larger aC^\pm than the other two sites (Table 3) because of the elevated equilibrium slope a (with C^\pm coefficients within the same range of variability at all three sites). Therefore, for the same magnitude wave event, the shoreline moves more quickly toward equilibrium at Camp Pendleton.

6. Discussion

6.1. Alternative Model Formulations

[32] Model results are similar when $E^{1/2}$ in (2) is replaced with E or E^2 (similar to the rate parameterizations suggested by Miller and Dean [2006]), or if the wave forcing is parameterized instead with wave height, Ω [Wright et al., 1985], or the radiation stress component S_{xx} (Figure 8). For different wave forcing, the model RMSE (across all eight sections at Torrey Pines beach) ranges from 3.3 to 5.2 m (E), 3.4 to 5.8 m (wave height), 3.3 to 5.8 m (radiation stress component S_{xx}), and 4.9 m to 8.2 m (Ω). Similar model performance with different wave parameterizations is

expected because time series of E are correlated with wave height (0.92), the radiation stress component S_{xx} (0.99), and Ω ($R^2 = 0.54$).

[33] Model free parameter values likely depend on sand grain size [Dean, 1977; Wright et al., 1985]. In a series of numerical studies of equilibrium beach profile change, Kriebel and Dean [1985, 1993] demonstrated that larger grain size beaches have shorter characteristic time scales and smaller erosion potential. For example, increasing the median grain size from 0.2 mm to 0.3 mm decreased change rates by a factor of 4 [Kriebel and Dean, 1993]. The sediment grain size (e.g., Table 1) could therefore affect the magnitude of the equilibrium slope a and the rate change coefficients C^\pm , which both affect the rate of beach change. Observations of shoreline location and hourly wave characteristics on beaches with different wave climates and sediment types would help establish the role of wave period and grain size (e.g., $\Omega = H_b/w_s T$, where w_s depends on grain size).

[34] Model RMSE are only slightly reduced when the coefficients C^\pm are allowed to vary with the msl position S , and the addition of more free parameters is not justified. In (2), shoreline change stops when either $E = 0$ or $\Delta E = 0$ (equilibrium is reached). With a linear equilibrium wave energy expression (4), the maximum accreted shoreline position occurs at $S_{\max} = -b/a$ (5). Asymptotic forms (e.g., tanh) of the equilibrium wave energy (4), with an additional free

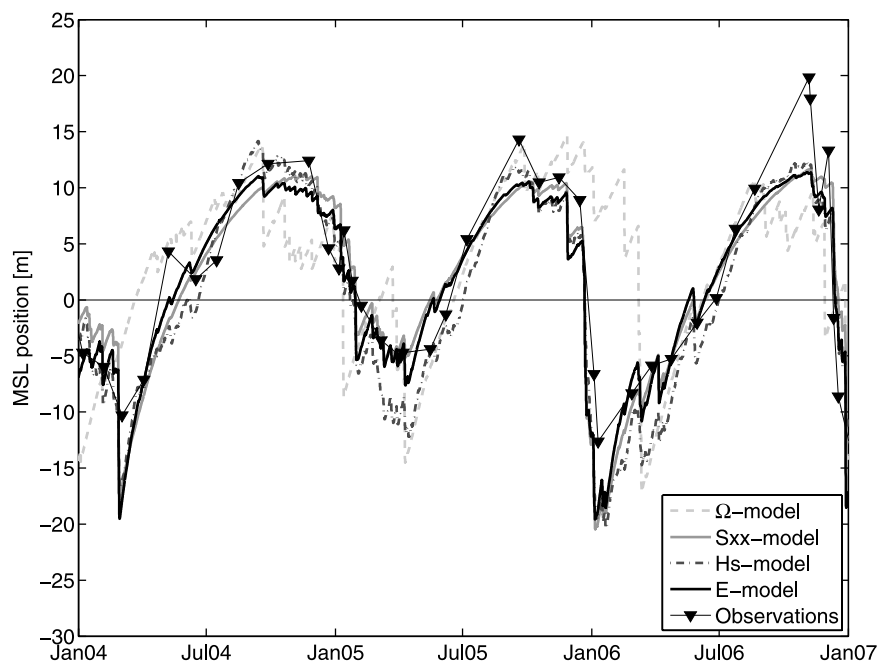


Figure 8. Observed and modeled msl position versus time for 3 years at Torrey Pines section T3. The model wave parameterizations are Ω (dashed light gray curve), wave radiation stress S_{xx} (solid medium gray curve), wave height H_s (dash-dotted dark gray curve), and wave energy E (solid black curve).

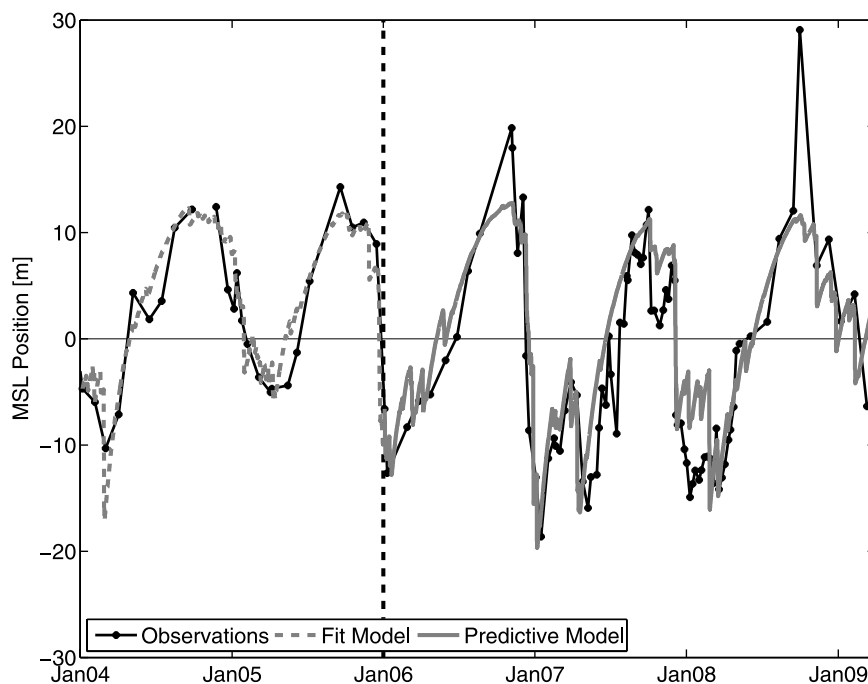


Figure 9. Two years of approximately monthly msl observations (solid black curve before the vertical dashed line) at Torrey Pines section T3 were used to determine the model free parameters, with the best fit RMSE = 2.8 m (dashed gray curve). Using the tuned free parameter values and the observed wave energy, an additional 3 years of weekly and monthly msl observations are predicted with RMSE = 4.7 m (solid gray curve). The anomalously large accretion event in September 2008 (present in alongshore sections T1–T4 and largest in T3) is not modeled and is unexplained.

coefficient, allow an asymptotic approach to equilibrium, eliminating the fixed maximum accreted msl position. However, the data did not significantly constrain this model refinement (not shown). Here, we present a simple model that is consistent with the observations and has relatively few free parameters.

6.2. Comparison to Miller and Dean's [2004] Model Results at Torrey Pines

[35] The Miller and Dean [2004] shoreline change model includes assumptions and effects (e.g., berm height and water level) that are not included in the present model. However, the models are similar in that both hypothesize that the msl position contour moves exponentially to a location that depends on present wave conditions, at a rate proportional to the disequilibrium between the present waves and shoreline location. A significant difference is that Miller and Dean [2004, equation (4)] formulate a specific dependence of the equilibrium shoreline location on water level, berm height, breaking wave height, and surf zone width. This dependence assumes an equilibrium beach profile with the water depth proportional to $x^{2/3}$, where x is the distance from the shoreline. In contrast, the present model determines the relationship between waves and the equilibrium shoreline location (4) from observations, resulting in four free parameters compared with three parameters given by Miller and Dean [2004].

[36] Prior to comparison with observations, Miller and Dean [2004, 2006] adjust the measured msl displacements

to account for volume losses on each profile and then detrend the msl location time series (but not the wave observations). Miller and Dean [2006] report (for 13 different change rate coefficient formulations) a maximum R^2 of 0.7. The present msl observations are not adjusted or detrended, and the present model shows improved agreement with the observations, with an average R^2 (over all eight alongshore sections) of 0.81, ranging from 0.66 to 0.94 (Figure 7d). It is unclear if the differences in model performance arise from the different model formulations, from the quality of the available 1974 wave data (Wave Information Studies (WIS) hindcasts shoaled assuming plane parallel depth contours), or from the different time periods studied.

6.3. Predicting Change

[37] Given free parameter values and the initial msl position, the model can be used to estimate msl position time series with only a wave energy time series. Model free parameters determined by fitting 2 years of msl position and wave energy observations at Torrey Pines (section T3) were used to predict 3 years of msl position with the observed wave energy. The model RSME, 2.8 m during the 2-year tuning period, increased to only 4.7 m during the 3-year prediction period (Figure 9). Short time scale (weekly to monthly) fluctuations were not predicted accurately in either the tuning or prediction periods. Maximum and minimum msl position were predicted within a few meters, except an anomalous accretion event during September 2008, which

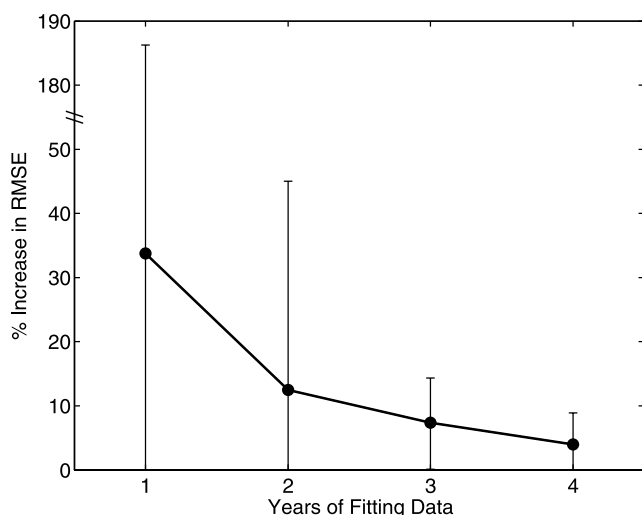


Figure 10. Percent increase in model RMSE above the baseline (using all observations at Torrey Pines) versus the number of years of monthly data used to tune the model free parameters. Scatter bars show the range of values obtained (note the vertical scale break), including variability from both different test periods and alongshore sections (for a total of 32 1-year tests, 24 2-year tests, 16 3-year tests, and 8 4-year tests).

was present in alongshore sections T1–T4 and largest (by a factor of 2) in section T3.

6.4. Sensitivity to Observation Duration

[38] A range of wave and beach change observations are required to determine the model free parameters. At Torrey Pines beach, it was necessary to survey for at least one full seasonal cycle (1 year) to span a typical range of beach and wave conditions. The model performance was then investigated using different observation durations (from 1 to 4 years) to estimate the model free parameters. The comparison baseline is the best model fit using all weekly to monthly observations for almost 5 years at each of the eight alongshore sections at Torrey Pines (e.g., section T3 in Figure 4).

[39] The observations were subsampled monthly to remove effects associated with weekly sampling, and the 4-year period from 2004 to 2008 was divided into consecutive 1-, 2-, 3-, and 4-year periods (for a total of four 1-year periods, three 2-year periods, two 3-year periods, and one 4-year period at each alongshore section). Thus, for 1-year tests, the model free parameters were determined with 1 year of data, and the RMSE was estimated for the entire nearly 5-year period. Each year was used for tuning at each of the eight alongshore sections, yielding 32 estimates of 1-year model tuning. Using only 1 year of data to fit the model, the RMSE increases only an average of $\sim 30\%$ above the baseline (Figure 10). No single year was the best or worst year for tuning in every alongshore section. An unexplained anomaly was noted at alongshore sections T5 to T7 when the year 2006 was used for tuning: the RMSE increases were a factor of almost three larger than all other tests. When 2 years of monthly observations were used for tuning, the mean RMSE decreases from 30% to less than 15%

above the baseline. Further increases in observation duration decrease the RMSE only slightly.

6.5. Sensitivity to Msl Survey Frequency

6.5.1. Monthly Versus Weekly Surveys

[40] From May 2007 to May 2008, Torrey Pines beach was surveyed weekly to resolve storm erosion events and subsequent beach recovery (Figure 4). The weekly observations were subsampled monthly, and the weekly and monthly time series of the same year were used to determine the best fit model free parameters for that year (not shown). Using the two sets of free parameter values, the RMSE for the entire 5 years of observations differed by only 1%. Weekly observations for 1 year did not improve significantly the model performance.

6.5.2. Biannual Surveys

[41] The model performance also was tested with biannual observations over an approximately 4-year period, simulating seasonal surveys, demonstrating how the model would perform with minimal observations of the msl seasonal cycle. The observations at each alongshore section at Torrey Pines were subsampled biannually, starting at different months in the year and resulting in six sets of biannual observations (e.g., January and July or February and August, etc., Figure 11). The optimal free parameters were determined for each set of subsampled observations, and the RMSE was calculated over the entire 5-year observation period. The mean RMSE (over eight alongshore sections) is only $\sim 25\%$ above the baseline for biannual surveys completed in January and July (similar to February and August and March and September, Figure 12). RMSE increases are larger for the remaining sets of biannual observations.

[42] Biannual sampling in February and August (Figure 11a, similar to January and July or March and September) constrains the model to fit the observations near the msl position extrema, with a RMSE only about 25% higher than using the entire weekly to monthly set of observations over the same time period. The May and November observations (e.g., Figure 11b, similar to April and October or June and December) do not constrain well the extrema in msl position because the November survey is often too early in the winter to capture the large erosion events, and the msl position has already begun to recover back to summer levels by the May survey. Summertime accretion is reproduced, but winter erosion is significantly overpredicted when the seasonal minimum beach width or a severe erosion event are not observed. Therefore, biannual observations are adequate to determine the model free parameters if they adequately sample the extremes in the range of msl position observations.

6.6. Sensitivity to Averaging Wave Energy

[43] The hourly wave energy E used here resolves the magnitude and timing of individual storm wave events, which are important for understanding beach change [Morton *et al.*, 1995; Lee *et al.*, 1998]. Averaging E over the time period between surveys (weekly to monthly) vastly simplifies the numerics of calculating optimal free parameter values but significantly degrades model performance by smoothing the wave history. In an example from Torrey Pines alongshore section T3, two 2-week-long wave energy time series $E(t)$ with the same 2-week average wave energy \bar{E} and

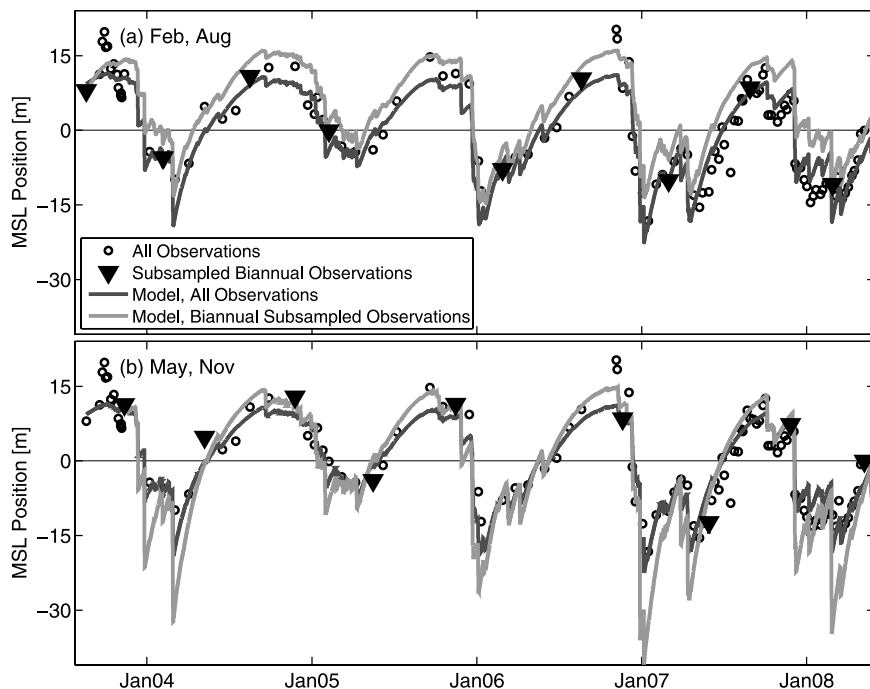


Figure 11. Msl position at Torrey Pines section T3 (with temporal mean removed) versus time. Circles are observations, with biannual subsamples indicated with bold triangles. The model tuned with all observations (RMSE = 4.0 m, dark gray curves) is compared to the model tuned with subsampled observations (light gray curves) for (a) February and August subsampling with RMSE = 4.6 m and (b) May and November subsampling with RMSE = 6.5 m.

approximately the same initial msl position S , yielded observed net msl changes of different signs (Figure 13). Larger than average wave energy events late in the 2-week period resulted in -2.3 m of net msl erosion in one case (Figure 13a),

while a large wave energy event early in the 2-week period followed by low-energy waves resulted in 2.1 m of net accretion in the second case (Figure 13b). If 2-week wave energy averages \bar{E} were used to drive the model, the two time

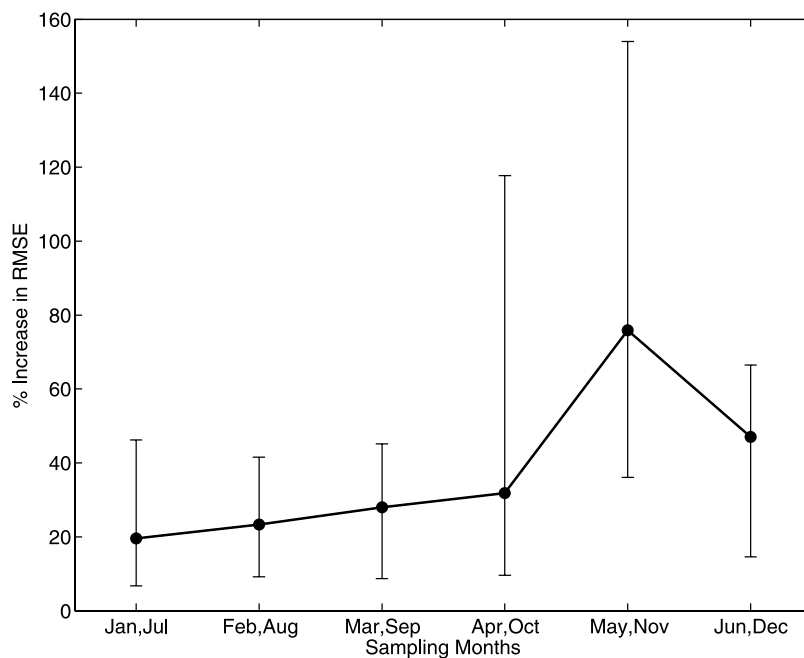


Figure 12. Percent increase in model RMSE above the baseline (using all observations at Torrey Pines) versus the 2 survey months of biannual surveys (separated by 6 months) used to tune the model free parameters. Scatter bars indicate the range of values for the eight alongshore sections at Torrey Pines.

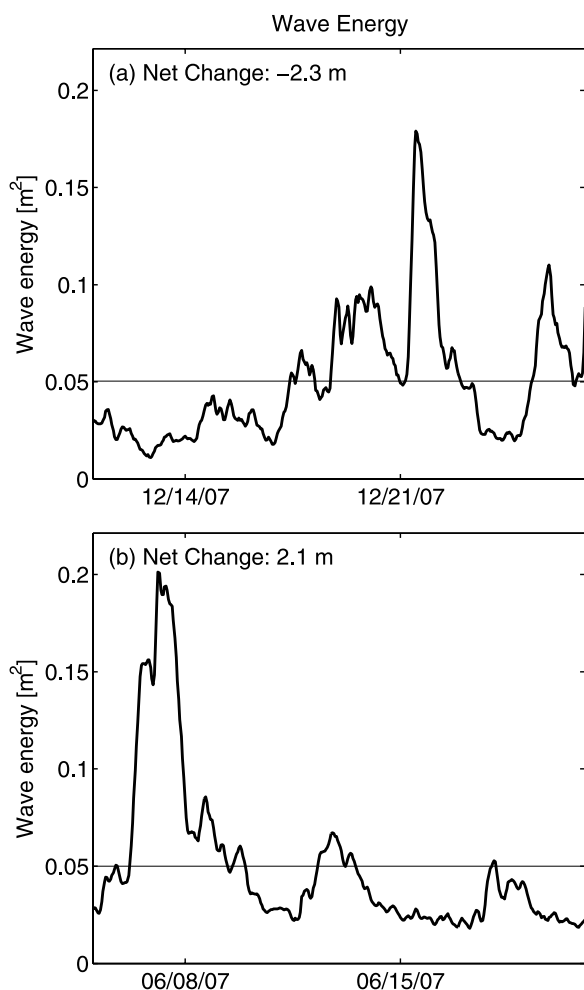


Figure 13. Hourly wave energy at Torrey Pines alongshore section T3 versus time for about 2 weeks between surveys in (a) December 2007 with -2.3 m of observed net erosion and (b) June 2007 with 2.1 m of observed net accretion. These time periods, with approximately the same initial msl position and average wave energy, yield observed msl change of opposite sign.

series would have the same effect and equal net msl changes would result.

[44] Averaging wave energy biases the estimated equilibrium wave energy E_{eq} . A synthetic hourly msl position time series, created using model output with optimal free parameters and observed hourly E at section T3, yields a clear separation between erosion and accretion events (e.g., E_{eq} , black line, Figure 14a). The hourly synthetic data were then averaged over the survey intervals. The averaging greatly reduces the maximum wave energy and erosion rates (compare Figure 14a with Figure 14b), introduces scatter by removing information about wave event timing (Figure 13), and biases the estimated E_{eq} (compare solid line (E_{eq}) in Figure 14a with dashed line (\bar{E}_{eq}) in Figure 14b).

[45] Using the averaged wave energy \bar{E} between the weekly to monthly surveys to determine (by minimizing the misfit with msl change observations) the averaged wave equilibrium energy \bar{E}_{eq} and the change rate coefficients \bar{C}^{\pm} , yields significantly larger errors (RSME between 6 and 12 m

for all eight alongshore locations) than obtained by optimization with hourly E (RSME between 3.2 and 5.2 m). Results for section T3 are shown in (Figures 15 and 4, respectively). When coupling the averaged E parameters with hourly wave energy, the model results are significantly degraded (RMSE between 9 and 31 m for the eight sections, and RMSE = 22.0 m, light gray curve, Figure 15). Although \bar{E} averaged over survey intervals qualitatively illustrates the equilibrium concepts (Figure 3), failure to resolve individual storms unacceptably degrades the model performance.

6.7. Extension to Include Shallow Depth Contours

[46] Equilibrium models are based on the implicit assumption that the entire beach profile, including near the shoreline (e.g., msl contour), responds coherently and predictably to changing wave conditions. Below, using alongshore-averaged contour changes, a significant portion of the msl and other contour changes at Torrey Pines are shown to be explained with the mode 1 EOF, showing the strongly coherent pattern of cross-shore profile change we believe is required for good model performance. This coherent pattern also suggests that the msl model can be readily extended to deeper contours.

[47] In addition to over 100 surveys of the subaerial beach used for msl studies, 16 bathymetry surveys covered all eight alongshore sections at Torrey Pines, spanning from the backbeach to approximately -9 m water depth (Figure 2a). The beach profiles show a large seasonal cycle (Figure 2c), consistent with the observations of *Winant et al.* [1975].

[48] The bathymetry changes are summarized with empirical orthogonal functions (EOFs) of contour locations. Time series of contour positions (-9 m to $+2$ m elevation, relative to msl) were estimated for each 500-m alongshore section. The temporal mean of each contour position was removed before computing the contour position EOF for each alongshore section. (Failure to remove the mean distorts the results significantly.) The seasonal, mode 1 EOF temporal amplitudes are similar to time series of msl position (Figure 16a) because msl and other contour motions are correlated. The mode 1 EOF spatial amplitudes (Figure 16b) describe the magnitude of the spatially coherent motion of each contour, showing that the offshore bar (-6 to -3 m elevation contours) and shoreline (-2 to $+2$ m) changes are out of phase. Thus, in summer when the shoreline is accreted, the bar contours are eroded, and the cycle reverses in winter.

[49] The contour position mode 1 EOF explains more of the fluctuations at some contours than others (Figure 16c). The fraction of contour displacement variance (R^2) explained by the mode 1 EOF is highest ($>50\%$) for the contours with the most change (e.g., largest spatial amplitudes, near the offshore bar and shoreline, black, Figure 16b). The mode 1 temporal EOF amplitude and msl position time series (Figure 16a) are similar, strongly suggesting that the equilibrium formalism used to model msl change at Torrey Pines can be extended to the entire profile using EOFs. Similar approaches may also be useful at sites with small or noisy msl position changes but coherent motion of deeper contours (e.g., Duck, North Carolina [*Quartel et al.*, 2008; *Alexander and Holman*, 2004]).

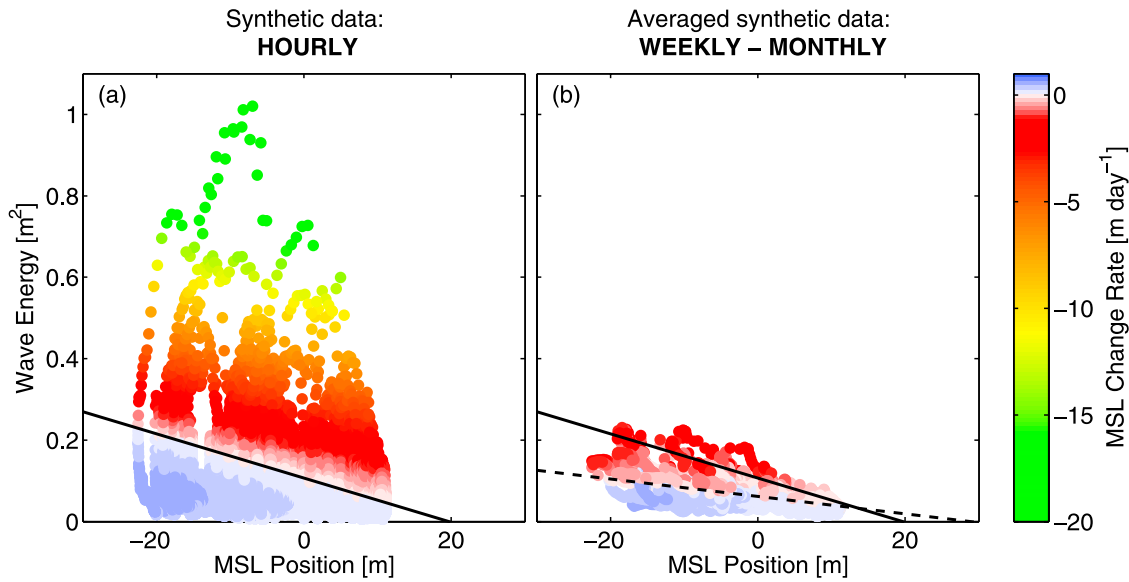


Figure 14. A synthetic time series of msl position change (created with model output using the optimal free parameters and wave energy time series at Torrey Pines section T3) shows the effects of using hourly E and weekly to monthly averaged \bar{E} to determine the equilibrium wave condition. (a) Hourly E and dS/dt and (b) weekly to monthly averaged \bar{E} and dS/dt . The “true” E_{eq} , determined with hourly E is the solid line in Figures 14a and 14b, and the dashed line in Figure 14b is the erroneous \bar{E}_{eq} obtained using averaged \bar{E} .

6.8. Model Applicability

[50] This simple shoreline change model performs well at three sites with large, seasonal msl contour movement (Figure 6). The model does not require a seasonal cycle, although a seasonal cycle provides a wide range of wave

conditions and msl locations to tune model parameters. On a beach with a strong seasonal cycle, the free parameters can be roughly approximated with 2 years of monthly observations or several years of biannual observations timed to include samples near an annual extreme in accreted and eroded msl

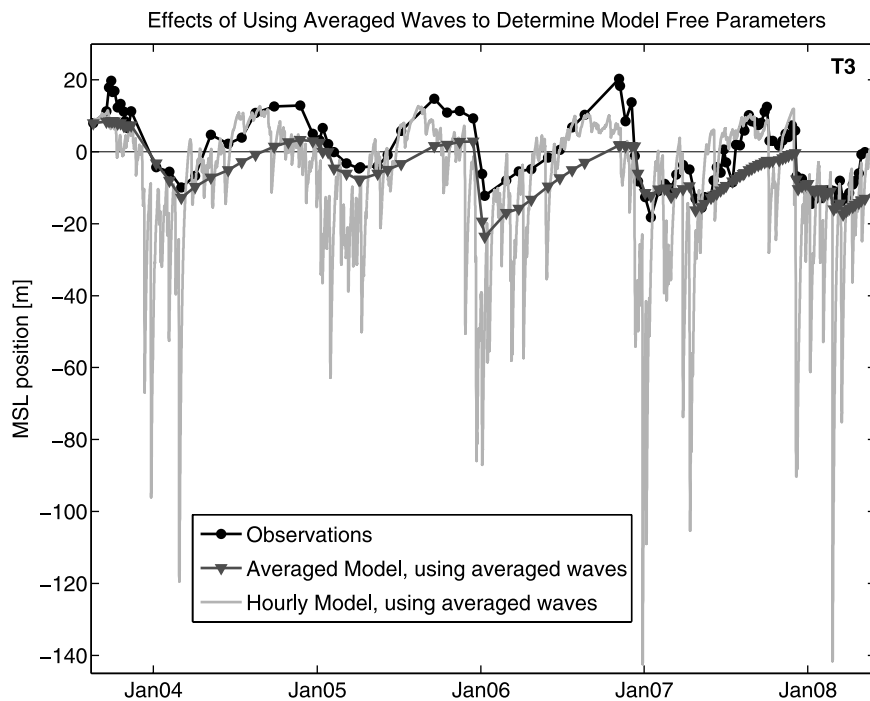


Figure 15. Msl observations (black curve) and wave-averaged model estimates at Torrey Pines section T3 versus time. Using \bar{E} averaged between the weekly to monthly surveys to determine the model free parameters significantly degrades the model estimates (RMSE = 7.5 m, dark gray curve, compared with RMSE = 4.0 m obtained using hourly wave energy in Figure 4). Coupling of the averaged \bar{E} parameters with the hourly E time series is even worse (RMSE = 22.0 m, light gray).

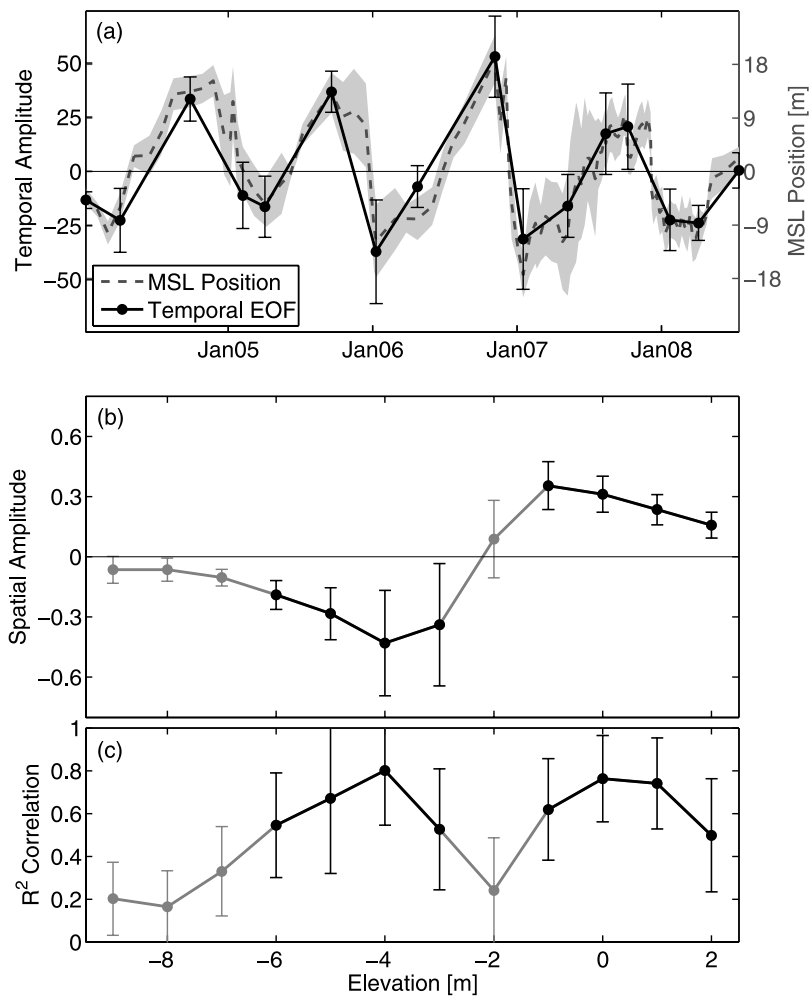


Figure 16. Changes in depth contour location are coherent over most of the depth profile at Torrey Pines. (a) Average (over all eight alongshore sections) mode 1 EOF temporal amplitude (black curve) is similar to the average msl position time series (dashed gray curve). The mode 1 EOF explains between 48 and 82% of the total variance at the eight alongshore sections. (b) Average mode 1 EOF contour position spatial amplitude and (c) average correlation R^2 between the mode 1 EOF temporal amplitude and each contour position time series. Shading (in Figure 16a) and scatter bars (in Figures 16a–16c) indicate the standard deviation between alongshore sections. In Figures 16b and 16c, black indicates $R^2 > 0.5$.

positions. Cobbles, bedrock, revetments, and cliffs, present to varying degrees at all the survey sites, clearly do not prevent good model performance, but their effect on model free parameter values is unknown. Using predetermined free parameter values for a site, the model can predict msl evolution given only the wave energy time series and the initial msl location. The model will be less reliable when extrapolated beyond the range of values used to determine the free parameters and will fail entirely if neglected geologic factors become important (e.g., underlying bedrock limits erosions, or sand availability limits accretion).

[51] The equilibrium model also assumes shoreline changes respond to wave energy and are insensitive to wave direction. This assumption is violated on beaches when a particular quadrant of wave approach drives convergence (or divergence) of the littoral drift, and hence accretion (or erosion).

[52] Previous work shows that shoreline change depends on elevated water levels (e.g., storm surge) [Larson and

Kraus, 1989; Kriebel and Dean, 1993]. Storm surge is small in southern California, owing to the narrow shelf, and water level is not included in the present model. Although msl location change for a given wave field likely depends on the tide level, more than three-quarters of all wave events over 2 m wave height lasted more than 6 hours, which is long enough to average the msl response to a given storm over a range of tide levels. Nevertheless, tide level does effect storm response, and additional observations resolving msl change during tidal cycles are needed to guide the inclusion of the effects of water levels.

7. Conclusion

[53] Shoreline location and wave energy observed for almost 5 years at Torrey Pines beach demonstrate the applicability of equilibrium beach change concepts [Wright et al., 1985; Miller and Dean, 2004]. The rate of cross-shore msl displacement depends on both the initial msl position and

the wave energy. A simple equilibrium shoreline response model with four free, tuned parameters reproduces the msl observations with relatively low RMSE (~ 5 m). The model performs similarly using alternative formulations of the wave forcing including wave height, Dean's parameter Ω , or the radiation stress component S_{xx} . The model also performs well at two nearby survey sites, each with about a year of observations. There was relatively little alongshore variability in the optimal free parameters within each survey site, and a single set of free parameters can reproduce the observations at most alongshore locations within each site with an approximate 10% increase in RMSE. Parameter variation between sites may result from variations in sediment grain size and availability. Additional observations during atypical years and at sites with different wave climates and sediments are being acquired to extend the model to include extreme conditions and more effects (e.g., sand grain size, wave period, and wave direction).

[54] **Acknowledgments.** Bathymetry and wave data collection were supported by the United States Army Corps of Engineers and the California Department of Boating and Waterways. Brian Woodward, Kent Smith, Dennis Darnell, Bill Boyd, and Ian Nagy built the bathymetry measuring system and completed the more than 200 surveys. CDIP, managed by Julie Thomas, maintained and operated the wave network. The vital contributions of the engineering and technical team are gratefully acknowledged. Marissa Yates was partially supported by a National Defense Science and Engineering Graduate Fellowship.

References

- Alexander, P. S., and R. A. Holman (2004), Quantification of nearshore morphology based on video imaging, *Mar. Geol.*, *208*, 101–111.
- Anthony, E. J. (1998), Sediment-wave parametric characterization of beaches, *J. Coastal Res.*, *14*(1), 347–352.
- Aubrey, D. G. (1979), Seasonal patterns of onshore/offshore sediment movement, *J. Geophys. Res.*, *84*, 6347–6354.
- Aubrey, D. G., D. L. Inman, and C. D. Winant (1980), The statistical prediction of beach changes in southern California, *J. Geophys. Res.*, *85*, 3264–3276.
- Bailard, J. A. (1981), An energetics total load sediment transport model for a plane sloping beach, *J. Geophys. Res.*, *86*, 938–954.
- Barth, N., and C. Wunsch (1990), Oceanographic experiment design by simulated annealing, *J. Phys. Ocean.*, *20*, 1249–1263.
- Booker, A. J., J. E. Inman, P. D. Frank, D. B. Serafini, V. Torozon, and M. W. Trosset (1999), A rigorous framework for optimization of expensive functions by surrogates, *Struct. Multidiscip. Optim.*, *17*, 1–13.
- Bruun, P. (1954), Coastal erosion and development of beach profiles, *Tech. Memo. 44*, U.S. Army Corps of Eng., Washington, D. C.
- Dalrymple, R. A. (1992), Prediction of storm/normal beach profiles, *J. Waterw. Port Coastal Ocean Eng.*, *118*, 193–200.
- Dean, R. G. (1973), Heuristic models of sand transport in the surf zone, paper presented at Conference on Engineering Dynamics in the Surf Zone, Inst. of Eng., Sydney, N. S. W., Australia.
- Dean, R. G. (1977), Equilibrium beach profiles: U.S. Atlantic and Gulf coasts, *Technical Report No. 12*, Department of Civil Engineering, University of Delaware.
- Dean, R. G. (1991), Equilibrium beach profiles: Characteristics and applications, *J. Coastal Res.*, *7*, 53–84.
- Dong, P., and K. Zhang (2002), Intense near-bed sediment motions in waves and currents, *Coastal Eng.*, *45*, 75–87.
- Drake, T. G., and J. Calantoni (2001), Discrete particle model for sheet flow sediment transport, *J. Geophys. Res.*, *106*(C9), 19,859–19,868.
- Dubois, R. N. (1990), Barrier-beach erosion and rising sea level, *Geology*, *18*, 1150–1152.
- Gallagher, E. L., S. Elgar, and R. T. Guza (1998), Observations of sand bar evolution on a natural beach, *J. Geophys. Res.*, *103*(C2), 3203–3215.
- Gourlay, M. R. (1968), Beach and dune erosion tests, *Delft Hydraulics Lab. Rep. m935/m936*, Delft, Netherlands.
- Hoefel, F., and S. Elgar (2003), Wave-induced sediment transport and sandbar migration, *Science*, *299*, 1885–1887, doi:10.1126/science.1081448.
- Hsu, T.-J., J. T. Jenkins, and P. L.-F. Liu (2004), On two-phase sediment transport: Sheet flow of massive particles, *Proc. R. Soc. London Ser. (A)*, *460*, 2223–2250, doi:10.1098/rspa.2003.1273.
- Inman, D. L., M. H. S. Elwany, and S. A. Jenkins (1993), Shorerise and berm profiles on ocean beaches, *J. Geophys. Res.*, *98*(C10), 18,181–18,199.
- Jiménez, J. A., J. Guillén, and A. Falqués (2008), Comment on the article “Morphodynamic classification of sandy beaches in low energetic marine environment” by Gómez-Pujol, L., Orfila, A., Ca nellas, B., Alvarez-Ellacuria, A., Méndez, F. J., Medina, R., and Tintoré, J., *Mar. Geol.*, *242*, 235–246, 2007, *Mar. Geol.*, *255*, 96–101.
- Kriebel, D. L., and R. G. Dean (1985), Numerical simulation of time-dependent beach and dune erosion, *Coastal Eng.*, *9*, 221–245.
- Kriebel, D. L., and R. G. Dean (1993), Convolution method for time-dependent beach profile response, *J. Waterw. Port Coastal Ocean Eng.*, *119*, 204–226.
- Larson, M., and N. C. Kraus (1989), SBEACH: Numerical model for simulating storm-induced beach change, *Tech. Rep. CERC-89-9*, U.S. Army Corps of Eng., Vicksburg, Miss.
- Larson, M., M. Capobianco, and H. Hanson (2000), Relationship between beach profiles and waves at Duck, North Carolina, determined by canonical correlation analysis, *Mar. Geol.*, *160*, 275–288.
- Lee, G., R. J. Nicholls, and W. A. Birkemeier (1998), Storm-driven variability of the beach-nearshore profile at Duck, North Carolina, USA, 1981–1991, *Mar. Geol.*, *148*, 163–177.
- List, J. H., and A. S. Farris (1999), Large-scale shoreline response to storms and fair weather, in *Coastal Sediments '99*, edited by N. C. Kraus and W. G. McDougal, pp. 1324–1338, Am. Soc. of Civ. Eng., Reston, Va.
- Marsden, A. L., M. Wang, J. E. Dennis, and P. Moin (2004), Optimal aerodynamic shape design using the surrogate management framework, *Optim. Eng.*, *5*, 235–262.
- Masselink, G., and A. D. Short (1993), The effect of tide range on beach morphodynamics and morphology: A conceptual beach model, *J. Coastal Res.*, *9*(3), 785–800.
- Miller, J. A., and R. G. Dean (2006), An engineering scale model for predicting the shoreline response to variations in waves and water levels, in *Coastal Engineering 2006: Proceedings of the 30th International Conference: San Diego, California, USA, 3–8 September 2006*, edited by J. McKee Smith, pp. 3554–3566, World Sci., Hackensack, N. J.
- Miller, J. A., and R. G. Dean (2007), Shoreline variability via empirical orthogonal function analysis: Part II. Relationship to nearshore conditions, *Coastal Eng.*, *54*, 133–150.
- Miller, J. K., and R. G. Dean (2004), A simple new shoreline change model, *Coastal Eng.*, *51*, 531–556.
- Morton, R. A., J. C. Gibeau, and J. G. Paine (1995), Meso-scale transfer of sand during and after storms: Implications for prediction of shoreline movement, *Mar. Geol.*, *126*, 161–179.
- O'Reilly, W. C., and R. T. Guza (1998), Assimilating coastal wave observations in regional swell predictions. Part I: Inverse methods, *J. Phys. Oceanogr.*, *28*, 679–691.
- Özkan Haller, H. T., and S. Brundidge (2007), Equilibrium beach profile concept for Delaware beaches, *J. Waterw. Port Coastal Ocean Eng.*, *133*(2), 147–160, doi:10.1061/(ASCE)0733-950X(2007)133:2(147).
- Pawka, S. S. (1983), Island shadows in wave directional spectra, *J. Geophys. Res.*, *88*, 2571–2591.
- Plant, N. G., R. A. Holman, and M. H. Freilich (1999), A simple model for interannual sandbar behavior, *J. Geophys. Res.*, *104*(C7), 15,755–15,776.
- Quartel, S., A. Kroon, and B. G. Ruessink (2008), Seasonal accretion and erosion patterns on a microtidal sandy beach, *Mar. Geol.*, *250*, 19–33, doi:10.1016/j.margeo.2007.11.003.
- Roelvink, J. A., and M. J. F. Stive (1989), Bar-generating cross-shore flow mechanisms on a beach, *J. Geophys. Res.*, *94*, 4785–4800.
- Swart, D. H. (1974), Offshore sediment transport and equilibrium beach profiles, *Tech. Rep. Publ. 131*, Delft Hydraulics Lab., Delft, Netherlands.
- Winant, C. D., D. L. Inman, and C. E. Nordstrom (1975), Description of seasonal beach changes using empirical eigenfunctions, *J. Geophys. Res.*, *80*, 1979–1986.
- Wright, L. D., and A. D. Short (1984), Morphodynamic variability of surf zones and beaches: A synthesis, *Mar. Geol.*, *56*, 93–118.
- Wright, L. D., A. D. Short, and M. O. Green (1985), Short-term changes in the morphodynamic states of beaches and surf zones: An empirical predictive model, *Mar. Geol.*, *62*, 339–364.

R. T. Guza, W. C. O'Reilly, and M. L. Yates, Scripps Institution of Oceanography, University of California, San Diego, 9500 Gilman Drive, La Jolla, CA 92093-0209, USA. (rguza@ucsd.edu; woreilly@ucsd.edu; myates@coast.ucsd.edu)